THE AMERICAN SOCIETY OF MECHANICAL ENGINEERS
345 E. 47 St., New York, N.Y. 10017

88-GT-31

An Investigation of Axial Pump Backflow and a Method for its Control

M. ABRAMIAN
J. H. G. HOWARD
Dept. of Mechanical Engineering
University of Waterloo
Waterloo, Ontario, Canada N2L 3G1

P. HERMANN
Sundstrand Aviation Operation
Rockford, IL

ABSTRACT

The flow field within an axial flow inducer pump near the blade leading edge was explored by laser-Doppler velocimetry to extend the previous studies of the recirculation zone which is observed at low flow rates. Although a considerable region of upstream reverse flow and swirl was observed, the recirculation zone within the impeller was of limited axial extent and was confined to the pressure side of the passage. In an attempt to reduce the flow reversal, a series of perforated disks were placed in front of the inducer. The optimum disk geometry produced minor changes in the pump performance. LDV measurements of the flow field ahead and behind the disk showed considerable reduction of the swirl velocity under reverse flow conditions, with the observed upstream swirl opposite to the inducer rotation.

INTRODUCTION

When the flow through a pump is reduced to 40-80% of its design flow rate, reverse flow and a subsequent prerotation occurs upstream of the impeller near the inlet casing wall. The exact flow rate at which this phenomenon occurs is a function of the impeller design characteristics (Kurian and Radha Krishna, 1974 and Tanaka, 1980). Further reduction of flow causes the region of reversed swirling flow to extend further upstream and towards the casing centerline. In addition to the energy losses, in a high suction specific speed pump, severe mechanical vibration may arise from flow instability resulting in the failure of the bearings and seals. This limits the pump operating range to flow rates near design.

According to the experimental investigations of several researchers, Schiavello and Sen (1980) and Tanaka (1980), at a certain flow rate below design, the lower axial velocity causes the flow to approach the impeller at stall flow angle of attack resulting in local separation at the leading edge of the impeller blade. At some lower flow rate, the increased back pressure causes reverse flow. The prerotation of the incoming flow is then induced by the reverse flow presumably through shear stress.

Several attempts have been undertaken to reduce the subsequent flow instabilities and pressure fluctuations by modifications to the inlet pipe of the pump impeller. Kasztejna, et al (1985) introduced a backflow recirculator upstream of a high suction specific speed centrifugal impeller. It consisted of an annular slot which received the swirling backflow emerging from the impeller, a set of straightening vanes in an annulus surrounding the inlet pipe, and a second slot which returned the unswirled flow back into the main flow stream. The overall effect of this device on the performance was found to be negligible, but it allowed stable operation of the pump at very low flow rates. Paulon et al. (1985) modified the inlet of a four bladed axial pump by adding a cylindrical separator at two radial positions and found considerable improvement on the overall pump performance at low flow rates.

The investigation described here is a continuation of a previous research project (Howard et al., 1987), which set out to study the flow field ahead of and within a high specific speed pump inducer (Traditional Ns=5500) under off-design conditions. The present study includes velocity measurements at additional locations within the inducer close to the leading edge. As an attempt to reduce the flow reversal and its propagation further upstream, a series of perforated disks (reverse-flow-catchers) was placed, one at a time, in front of the inducer. Their effect on local flow stability (unsteadiness) and the overall pump performance is examined by performance tests, flow visualization, and velocity measurements at low flow rates and at various locations with respect to the inducer. The disk design has a minimized axial length, which is often a necessity for pumps in aircraft fuel system. The design attempts to minimize losses for flows into the pump and maximize losses for the reverse flow. A single component laser-Doppler velocimetry system, which allowed computation of the shaft-angle-averaged[1] statistics of the velocity, was employed to describe the flow field within and ahead of the inducer.

EXPERIMENTAL APPARATUS

Test Rig and Pump Inducer

The schematic diagram of the test rig is shown in Figure 1. It is a closed circuit arrangement using water as the working fluid. For the present study, since more losses were expected due to the presence of the flow-catchers, a boost pump was added in series with the test pump to enable the system to operate well above the pump design flow rate. Water was drawn by the inducer, through one of the venturis to the 127mm inlet pipe which was then collected by a spiral volute and returned to the tank through the boost

[1] Ensemble averaging the velocity with respect to the angular orientation of the rotating shaft.

Presented at the Gas Turbine and Aeroengine Congress
Amsterdam, The Netherlands—June 6-9, 1988

pump and a butterfly valve which controlled the flow. The inlet pipe which served as the inducer shroud and extended about 1.1 diameters upstream was manufactured from clear plastic to allow flow visualization. Static pressure taps were located on the shroud at different axial lengths upstream and downstream from the inducer. Flow visualization was made possible by introducing flow tracers or injecting dye through the static pressure taps.

The axial flow inducer is shown in Figure 2 and a detailed specification of its design parameters and geometry is given in Table (1).

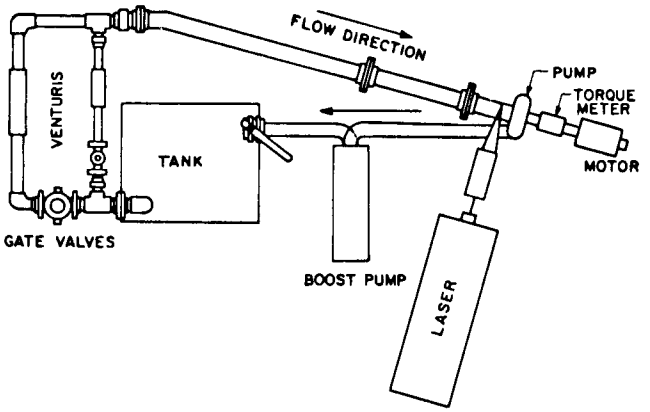

Figure 1: Schematic diagram of the test apparatus

Table 1: Inducer Design Parameters and Geometry

Design Flow Rate	11.04 l/s (175 GPM)
Design Speed	1700 RPM
Design Head	1.94 m (6.45 ft) H20
Tip Dia.	126 mm (4.95 in.)
Hub Inlet Dia.	38 mm (1.50 in.)
Hub Exit Dia.	64 mm (2.50 in.)
Axial Length	89 mm (3.50 in.)
No. of Blades	2
Blade Solidity	3.0 (tip) 2.2 (hub)
Blade Thickness	3 mm (0.125in.)
Entry Tip Blade Angle	7.5 *Degrees**
Exit Tip Blade Angle	12.23 *Degrees**
Blade Leading Edge Cone Angle	7 Degrees From Radial

* From tangential

Table 2: Flow-Catchers Parameters

Type	Radial Width (mm)	# of Holes	Density	Blockage/ Pump Entry Area
FC80	35.56	130	0.453	0.430
FC40	17.78	76	0.394	0.320
FC5	6.35	40	0.263	0.154
FC40NH	17.78	0	0.000	0.529

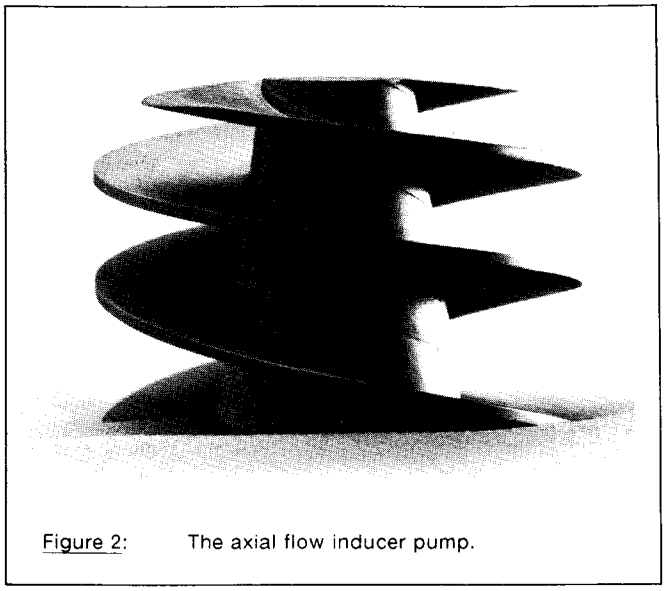

Figure 2: The axial flow inducer pump.

Reverse-Flow-Catchers

The four reverse-flow-catchers are shown in Figure 3. Each disk extends to the inlet tip diameter and covers a percentage of the inducer blade height at the inlet. To minimize losses in the normal flow direction, the holes in 6.53 mm (0.25 in.) thick disks were constructed with an aspect ratio (hole diameter/disk thickness) of 1.0 and a bevel (60 deg. total angle) on the upstream sides of the disks, as suggested by data from Miller (1971) and Idel'chik (1966).

Four different disks were employed. Three include holes and cover 80,40, and 5% of the inducer blade height at the inlet and one covers 40% of the inducer blade without holes. The holes are concentrically arranged 2.54 mm (0.1 in.) radially apart from each other with different angular distribution for each set. The disk labelled FC80 extends over 80% of the inducer inlet blade height and has holes at four radial locations. The disk FC40 covers 40% of the blade height with two rows of holes while FC5 extends over half the first set of holes and 5% of blade height. The fourth disk, FC40NH, has the same dimension as FC40 but no holes.

The area density of each flow-catcher (effective hole area / flow-catcher annulus area) and their geometry are summarized in Table (2). All flow-catchers were held inside the plastic shroud at 1.58 mm upstream from the inducer inlet during performance tests and flow visualization. During the LDV measurements the FC40 flow-catcher was held at 12.7 mm upstream from the inducer to allow the measuring control volume to penetrate from the shroud to the hub.

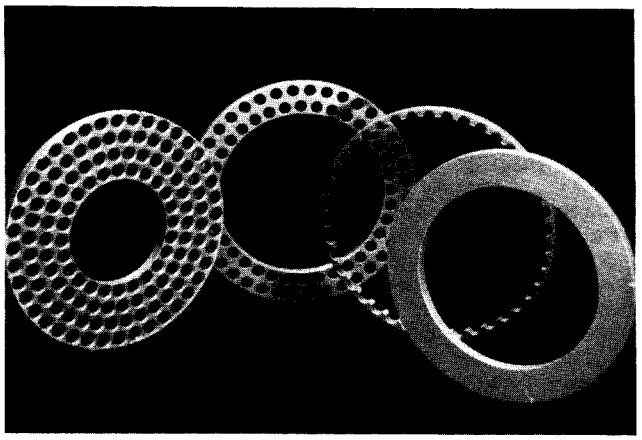

Figure 3: The Reverse-Flow-Catchers

MEASUREMENT PROCEDURE

The LDV system used for velocity measurements consisted of a 2W Ar-ion laser with single component transmitting and receiving optics which operated in backscatter mode. A single Bragg cell and electronic downmixing was used to provide the frequency shifting necessary to detect reverse flow. Two (axial and swirl) velocity components were obtained by rotating the optics. Details of the LDV system and data processing are given by Howard et al. (1987). In order to determine the extension of the reverse flow region inside the inducer, without any flow-catcher in place, shaft-angle-averaged measurements of both axial and swirl velocities were conducted at 4 axial locations (Z=0, -5.3, -8.3, -10.6 mm see Figure 4). At each axial location velocities were obtained at 6 radial positions (R/Rtip=0.48, 0.58, 0.69, 0.79, 0.9, 0.94). With the FC40 flow-catcher in place, radial mean profiles along with shaft angle averaged profiles of both (axial and swirl) components were measured at 6.5mm upstream and downstream of the flow-catcher, with the latter position between flow-catcher and inducer. A 250 mm focal length transmitting lens was employed to reduce optical obstruction by the inducer blades and to allow beam penetration through a plane, rectangular, high quality silica-glass window 16 mm wide. The window extended from Z=25 to -40mm and was placed close to the cylindrical inner shroud contour to minimize the effect of window flatness on the shroud curvature. The optimum combination of the lens focal length and the width of the glass window resulted in negligible effect of the flatness of the window on the shroud curvature. The LDV counter processor was permitted to make multiple measurements per burst. The signals were time-averaged at a given frequency which was varied depending on the data rate. The measurement error was estimated from the (radially) integrated axial velocity profile at design flow rate which agreed with the volume flow rate (as read from the venturi) within 0.5% for the upstream and within 2% for the downstream profile. Measurement accuracy was estimated to be within $\pm$0.1 m/s at all times.

The overall pump performance was determined by measuring the flow rate, total head rise, and torque at 1700 rpm (design). The flow rate was determined by measuring the pressure drop across two previously calibrated small and large venturis. The pump total head rise was determined by measuring the static pressure at the volute exit against the supply tank which was then converted to total pressure assuming uniform velocity distribution across the pipe. A comparison between the converted static pressure and the weighted average total head measurements at the exit of the volute showed a negligible difference of 0.1% over the entire range of the flow rates. A calibrated total head loss through the venturis and pipes up to Z=135mm (see Figure 4) was then added to the measured value to produce head rise from the pump inlet. Pressure was measured using a (0-138 kPa) variable-reluctance, differential pressure transducer. Torque was measured by a rotary transformer torquemeter located between the pump and the DC motor. All (pressure and torque) signals were time-averaged which allowed repeatability within 0.07 kPa for the pressure, and 0.05 Nm for the torque measurements. The pump was operated at all times with inlet pressure high enough to avoid observable cavitation.

Flow visualization studies were conducted at three (82,46, and 33) different percentages of inducer design flow rate by injecting dye through a stainless steel tubing inserted into the static pressure tap located at Z=42mm.

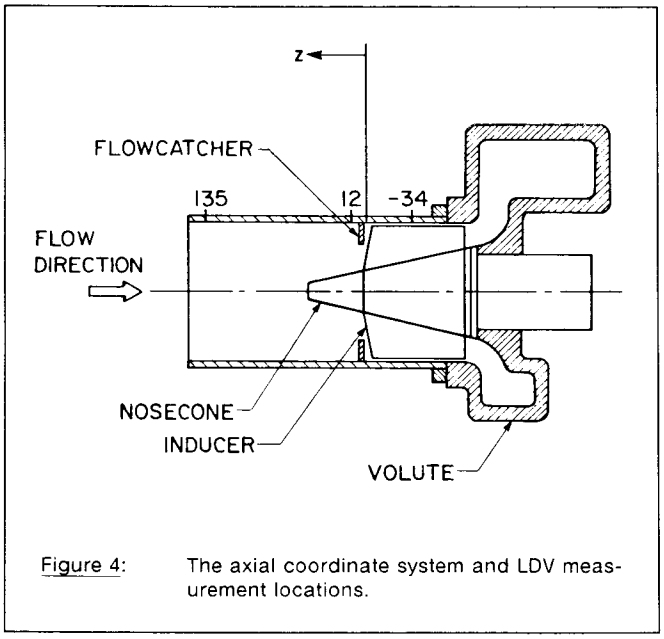

Figure 4: The axial coordinate system and LDV measurement locations.

RESULTS AND DISCUSSIONS

Flow description within the inducer

The shaft-angle-averaged absolute velocity data measured at 50% design flow rate and without any flow-catcher are presented, in the form of vector plots, in Figures 5,6, and 7 for Z=0, -5.3, and -10.6 mm respectively. The direction of the impeller rotation is from left to right and the angular coordinate on the graph increases in that direction. The graphical system shows the first measured location on the right and the last on the left which distributes the vectors between the suction and pressure sides of the passage.

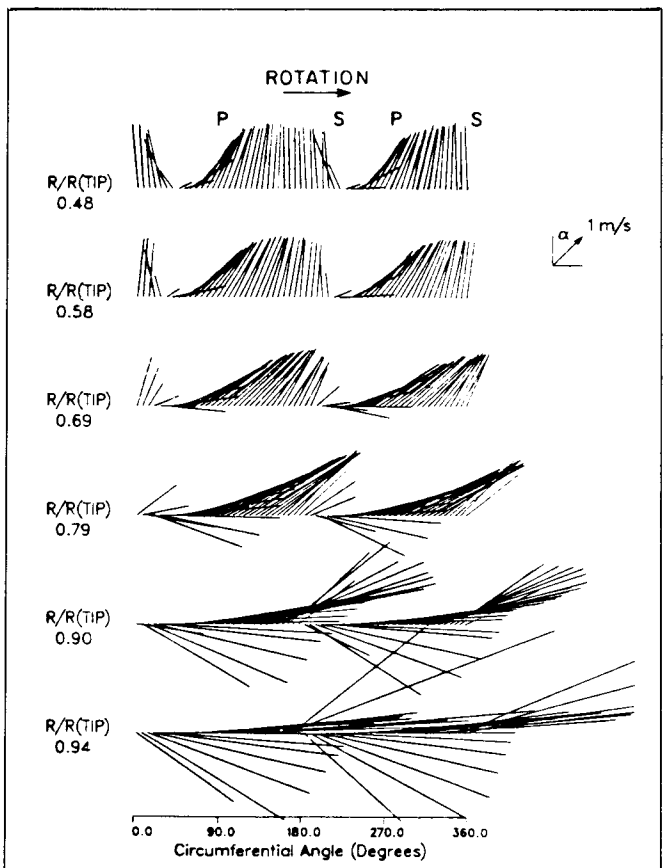

Figure 5: Shaft-angle-averaged absolute velocities at Z=0 and 50% flow rate; S: Suction side, P: Pressure side.

Arrowheads have been left off the vectors to avoid clutter. The base of each vector starts from the common origin line. Measurements very close to the blade surfaces were prevented by the blockage of one laser beam by the blade. At the plane of the hub leading edge (Z=0), reverse flow exists near the tip and is (radially) extended to its maximum towards the hub. The radial extension then decreases further downstream from the leading edge. Figure 8 summarizes the reverse flow region observed from the present and previous measurements (Howard et al., 1987), at 50% flow rate. The reverse flow region is observed to occupy only a limited axial distance past the blade leading edge and does not extend across the blade passage. According to the description of the graphical system given above, it should be noted that the reverse flow region is confined to the pressure side of the passage rather than the suction side. The pressure side separation has also been measured by Carey et al., (1985) at the entry of a mixed-flow pump. The separation was claimed to be associated with the large angle of incidence at the tip. However, if the occurrence of the reverse flow, at low flow rates, is due to the higher incidence of the incoming flow, the stall and separation would be expected on the suction side of the passage. At present, a flow model which will describe the pressure side reverse flow region has not been developed.

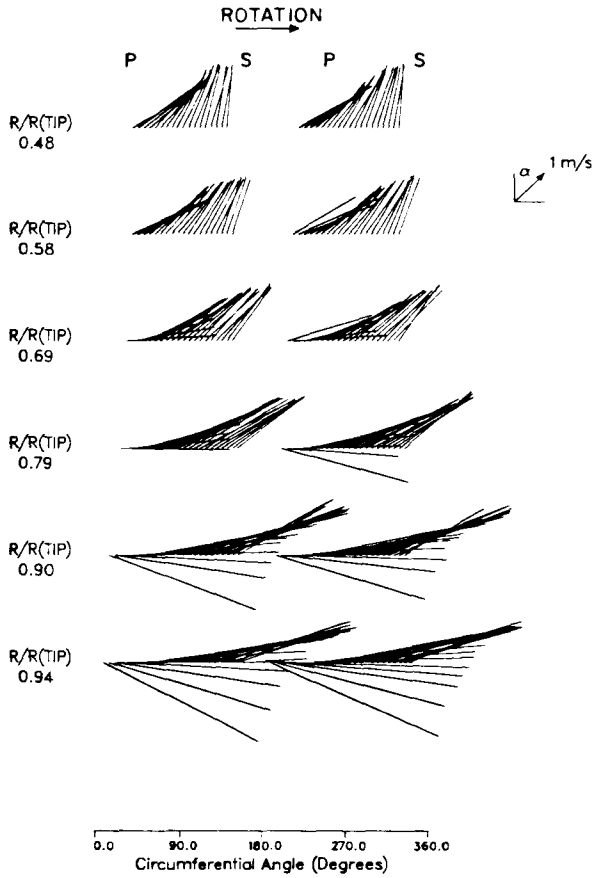

Figure 6: Shaft-angle-averaged absolute velocities at Z=-5.3 and 50% flow rate; S: Suction side, P: Pressure side.

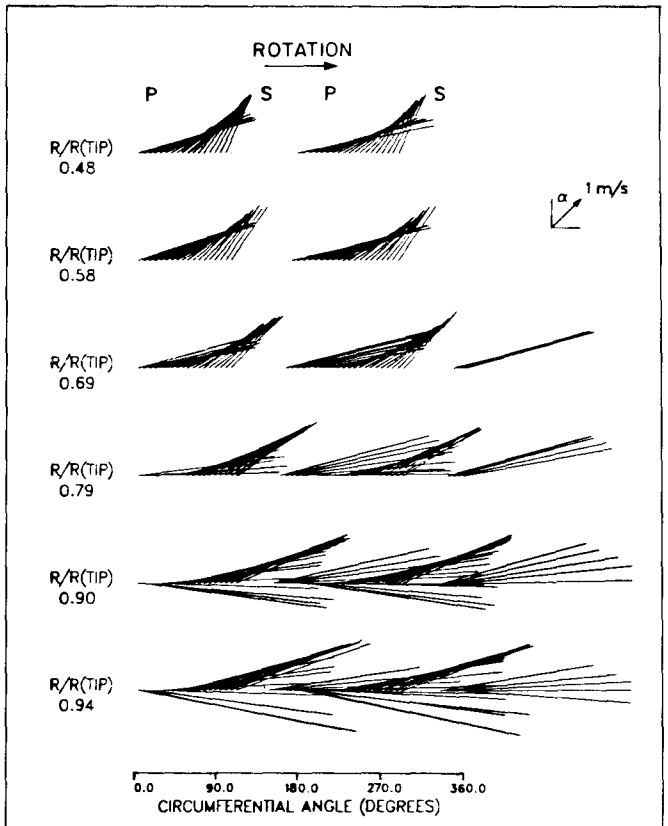

Figure 7: Shaft-angle-averaged absolute velocities at Z=-10.6 and 50% flow rate; S: Suction side, P: Pressure side.

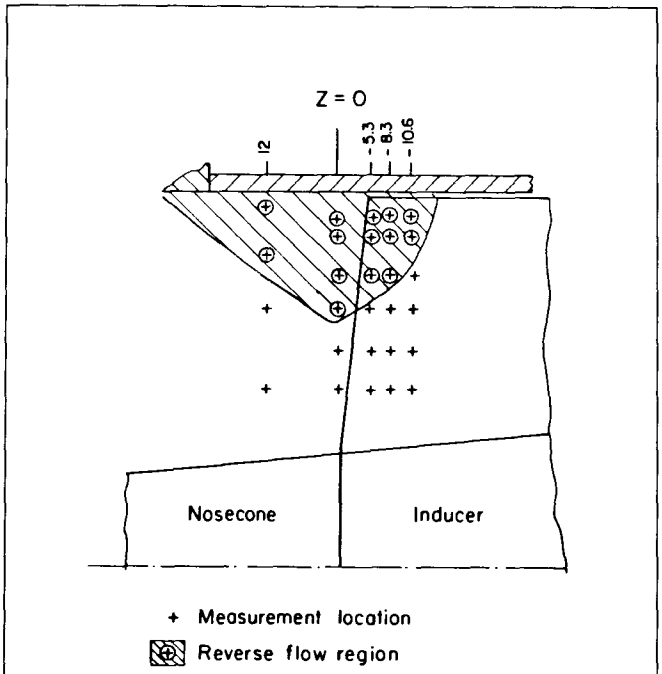

Figure 8: Reverse flow region within and ahead of the inducer at 50% flow rate.

Effect of flow-catchers on the inlet flow

Figures 9 and 10 present radial distribution of both axial and swirl velocities, upstream and downstream of the FC40 flow-catcher disk, at design and 50% of design flow rate. At design flow rate and upstream of the flow-catcher its presence has little effect, while downstream of the disk some positive swirl exists between it and the impeller. At 50% of design flow, however, a small negative swirl is generated upstream of the disk while a greatly increased positive swirl exists between the flow-catcher and the inducer. At the lower flow rate, the reverse (axial) flow downstream of the flow-catcher penetrates upstream through the hole near the tip but the overall upstream axial flow is positive. The shaft-angle-averaged data (Figures 11 & 12) also exhibit the negative swirl and the positive axial flow near the tip upstream of the disk. They also indicate that the periodic (blade passing) unsteadiness of the absolute flow near the tip is damped by the flow-catcher and has less amplitude further upstream.

The occurrence of the unexpected upstream reverse swirl phenomena was verified by flow visualization studies. The observations made at 46% of design flow rate clearly indicated that the FC40 disk resulted in upstream swirl opposite to the direction of the inducer rotation. The FC40NH flow-catcher, however, had no effect on the direction of the swirl. It may be concluded that the reverse flow through the holes results in flow separation and reattachment, which may act as a series of guide vanes and turn the flow in the direction opposite to the inducer rotation. The "local unsteadiness" or unsteadiness of the flow field was also observed. With a flow-catcher in place, the upstream streaklines, generated by injected dye, were quite well-behaved and steady from the shroud to the hub. Without a flow-catcher, the observed flow was unsteady at most radial locations. The kinetic energy of the upstream reverse flow was reduced by 52% from that observed without the disk at the same radial extension. The kinetic energy of the upstream swirl velocity, in the region of the reverse flow, was reduced by 90% from that observed without the disk and the swirl direction was changed.

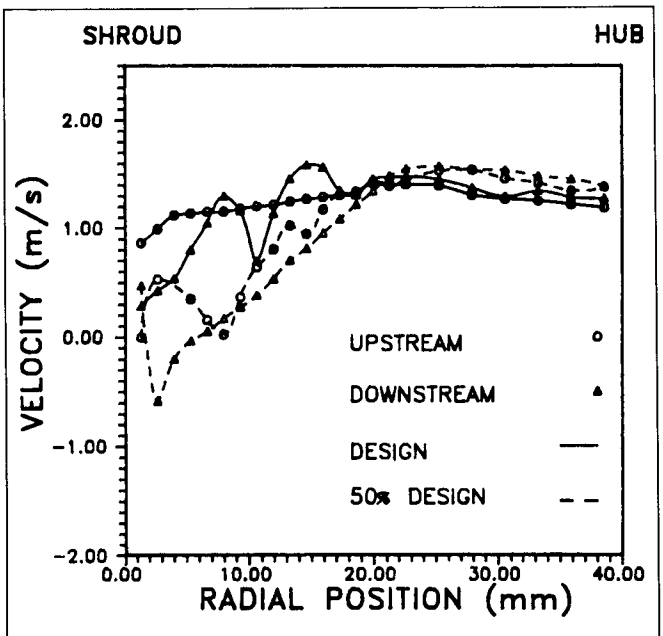

Figure 9: Radial distribution of axial velocity at design and 50% flow, upstream and downstream of the FC40 flow-catcher.

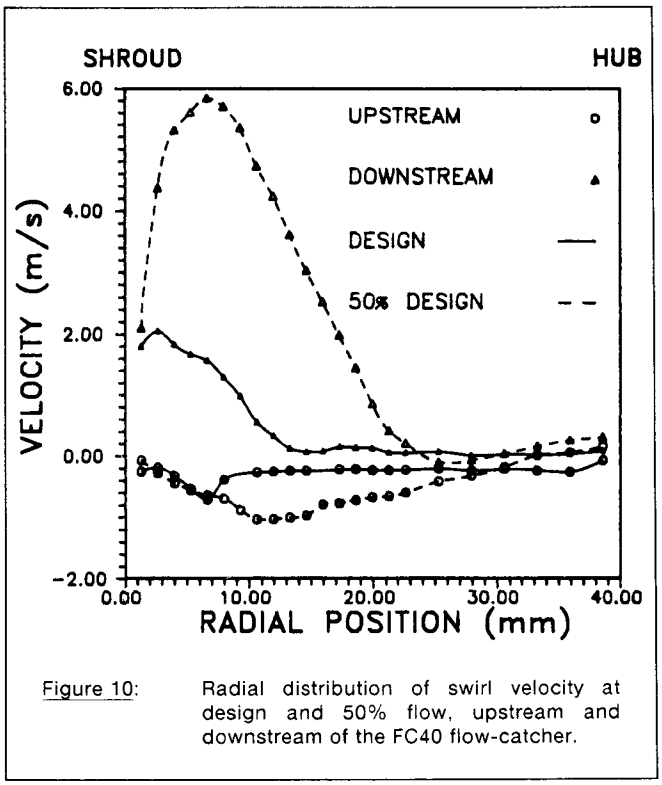

Figure 10: Radial distribution of swirl velocity at design and 50% flow, upstream and downstream of the FC40 flow-catcher.

Effect of flow-catchers on performance

The effect of the flow-catchers on the overall pump performance is presented in Figures 13, 14, and 15, for efficiency, head, and torque vs flow rate, respectively. The FC5 had a negligible effect on either the direction of the upstream swirl or the performance. Overall, due to higher blockage, all flow-catchers resulted in lower efficiencies near and above design flow rate. At very low flow rates (near shut-off), the head-flow characteristic of the pump is improved significantly by the FC40 disk, but the torque-flow characteristic is affected in the opposite manner. With the FC40 higher torques are exerted on the inducer than without any flow-catcher. This trend is reversed (lower head and lower torque) when the pump is fitted with the FC40NH flow-catcher. With the perforated disks, the increase in torque is compensated by the higher total head, resulting in no significant improvement on the overall efficiency of the pump. In relation to the flow visualization and flow measurement results, it seemed that the reverse swirl associated with the presence of the holes was responsible for the higher torques exerted on the inducer when fitted with the perforated flow-catcher.

In an attempt to control the direction of the swirl, the FC40 flow-catcher was tilted around its vertical centerline axis. The gaps around the shroud wall, created by tilting the disk, were sealed to prevent the reverse (axial) flow from penetrating upstream. Flow visualization studies conducted at a tilt angle of 16 degrees showed continuous positive swirl at all radii and low flow rates except at shut-off where two counter-rotating vortices were observed at the top and bottom portions of the shroud. This "angled" configuration did result in 2-3% less torque at low flow rates which was again compensated by the lower head rise with no significant improvement to the overall efficiency. Indeed, its higher blockage resulted in lower efficiencies than the "normal" FC40 near the design flow rate.

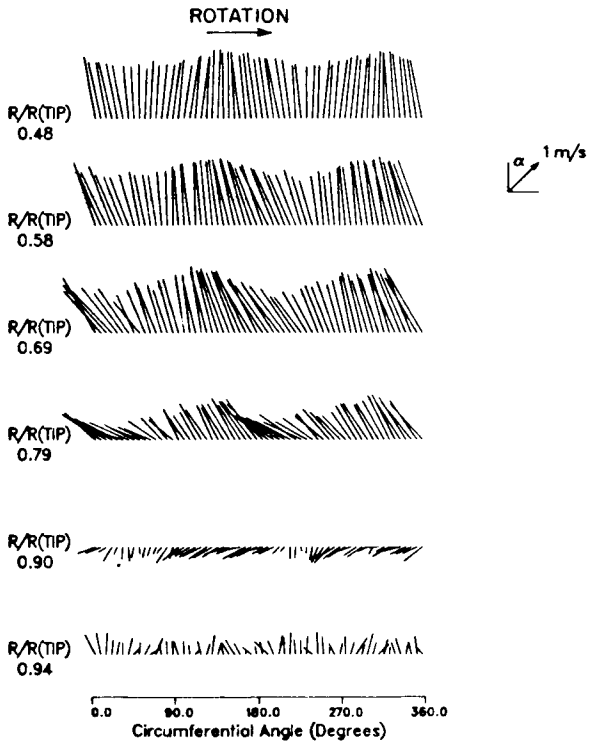

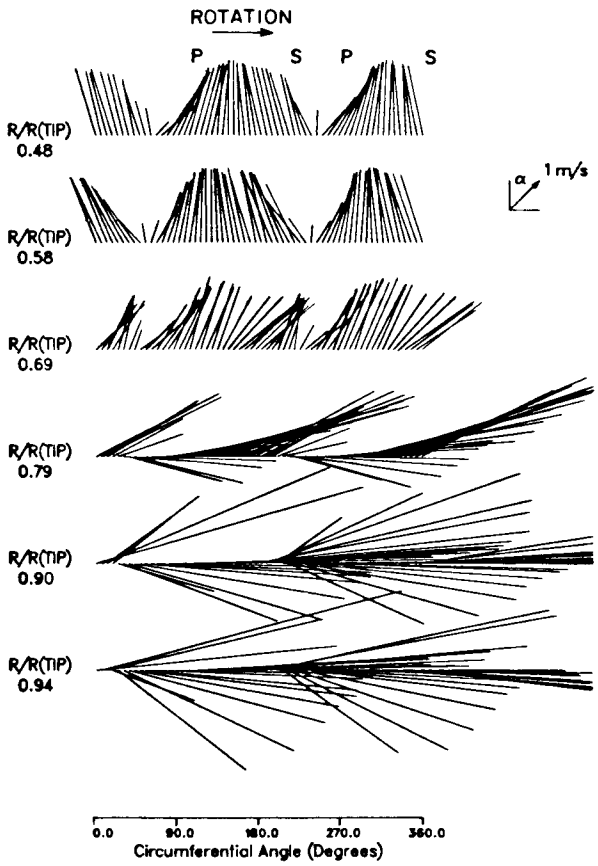

Figure 11: Shaft-angle-averaged absolute velocity at 50% flow, upstream (top) and downstream (bottom) of the FC40 flow-catcher. S: Suction side, P: Pressure side.

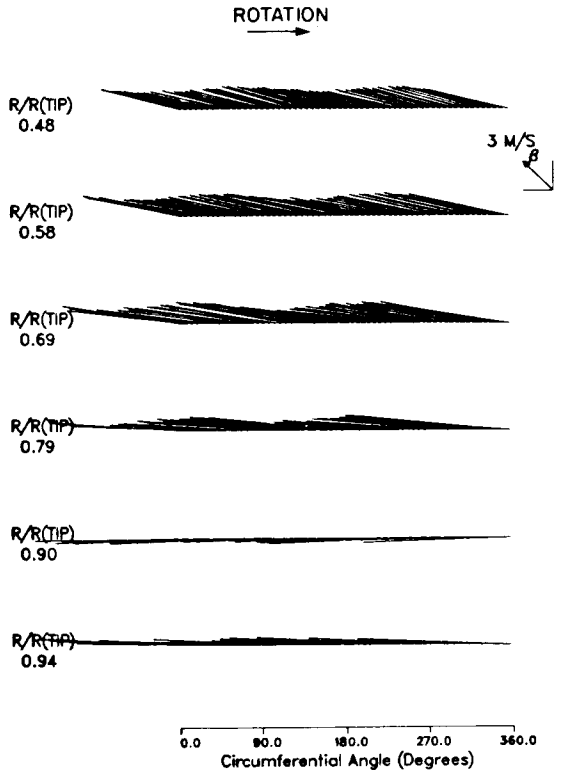

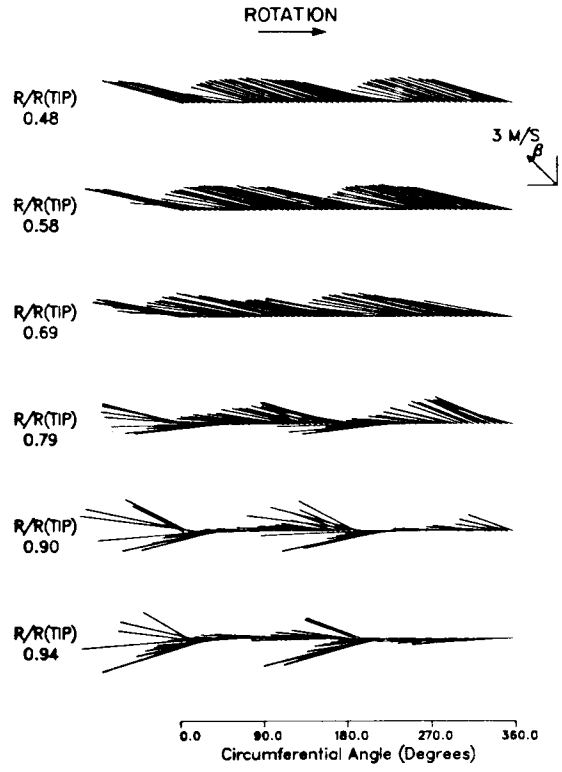

Figure 12: Shaft-angle-averaged relative velocity at 50% flow, upstream (top) and downstream (bottom) of the FC40 flow-catcher.

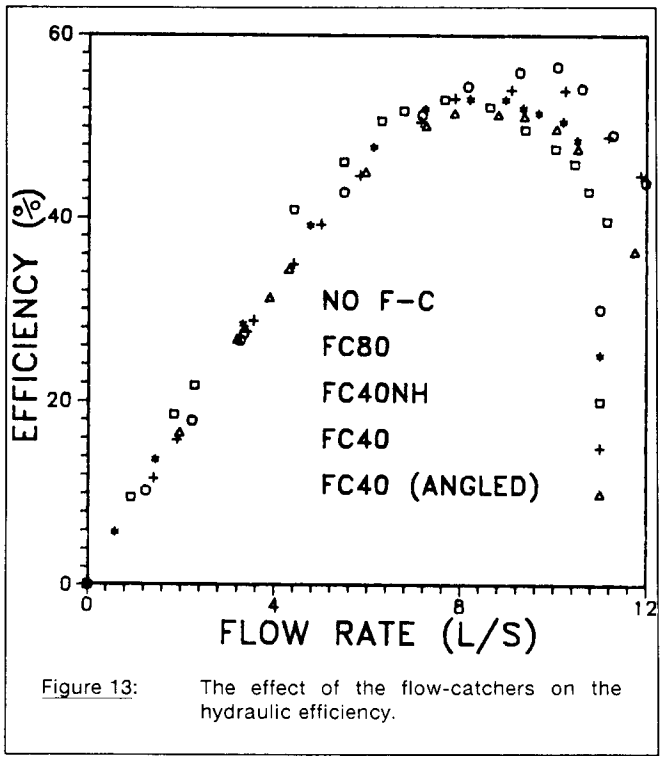

Figure 13: The effect of the flow-catchers on the hydraulic efficiency.

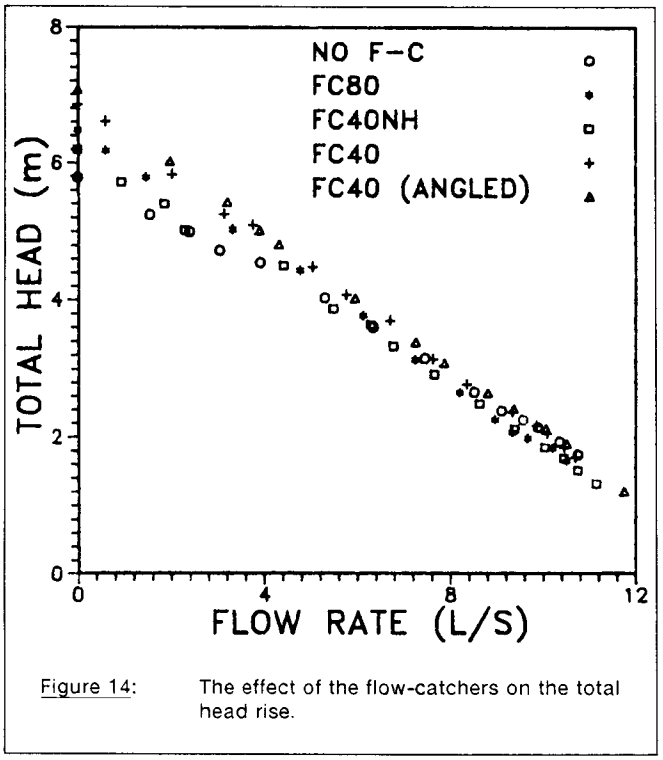

Figure 14: The effect of the flow-catchers on the total head rise.

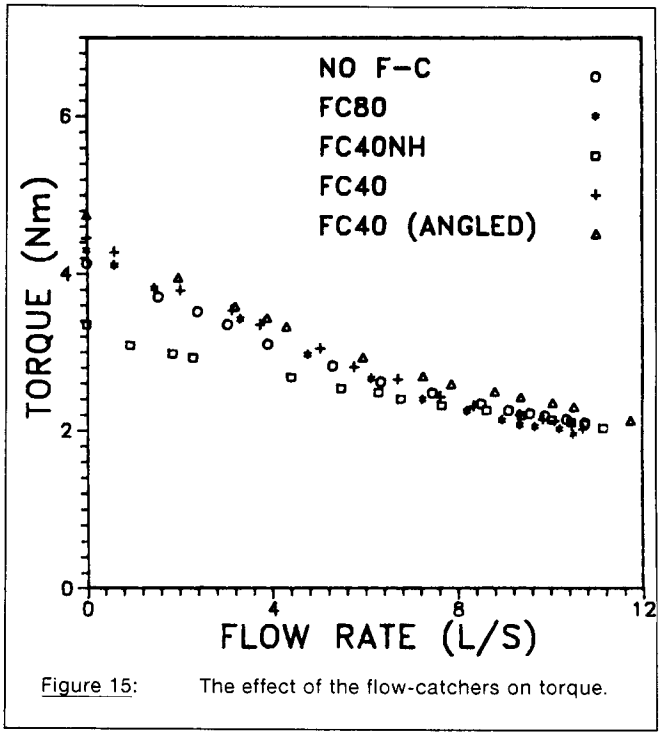

Figure 15: The effect of the flow-catchers on torque.

CONCLUSIONS

In the present study, velocity field measurements with LDV have extended the previous description of the recirculation zone at the entry tip region of an axial-flow inducer pump. Although a considerable region of upstream reverse flow and swirl was observed, the recirculation zone within the impeller was of limited axial extent and was confined to the pressure side of the blade passage. The complex flow fields close to the impeller leading edge and within the reverse flow zone are worthy of further study.

A perforated disk was placed immediately upstream of the inducer to modify or control the reverse flow and swirl. This form of "reverse-flow-catcher" has the advantage of a minimum axial length, which is important in some applications. Performance tests with several disk configurations indicate that the best geometry of those tested extended over 40% of the entry blade height. The disk has a very small adverse effect on head and efficiency at the pump design flow rate, but at lower flows, head and torque are increased with efficiency remaining unchanged.

The relationship between flow fields upstream and downstream of the disk is clarified by flow visualization observations and the laser velocity measurements. A trapped swirl region was observed between disk and impeller even at design flow. Placing the disk at an angle removed the reverse swirl but increased the blockage effect at higher flow rates.

A perforated disk similar to the tested form should have potential for the reduction of upstream reverse flow and swirl in pumps where axial length limitations are important. It should probably be placed as close as possible to the inducer leading edge. Further investigation is needed to determine cavitation or other two-phase flow effects.

ACKNOWLEDGEMENTS

Part of the experimental work reported here was carried out under a contract from Sundstrand Corporation whose permission to publish this paper is gratefully acknowledged. Support was also provided by a grant from the Natural Science and Engineering Research Council of Canada. The authors gratefully acknowledge the advice and assistance of Dr. Ing. C. Tropea. K. Lunau and D.L. Miller assisted with some measurements.

REFERENCES

Carey C., Fraser S.M., Rachman D., and Wilson G., 1985, "Studies of the Flow of Air in a Model Mixed-Flow Pump by Laser Doppler Anemometry," Report No. 699 Part 1&2, National Engineering Laboratory, East Kilbride, Glascow.

Howard J.H.G., Tropea C., Almahroos, H.M. and Roeber, T.W., 1987, "LDV Measurements of the Axial Velocity Field Within and Ahead of an Axial Pump Inducer at Off-Design Flow Rate," Proceedings of the ASME/JSME Thermal Engineering Conference, Vol.2, pp. 63-69.

Idel'chik, I.E., 1966, Handbook of Hydraulic Resistance. Translated from Russian by Barouch A. for the U.S. Atomic Energy Commission and National Science Foundation, p.144.

Kasztejna, P.J., Heald, C.C. and Cooper, P., 1985, "Experimental Study of the Influence of Backflow Control on Pump Hydraulic-Mechanical Interaction," Proceedings, 2nd Second International Pump Symposium, Houston, Texas, pp.33-40.

Kurian, T. and Radha Krishna, H.C., 1974, "A Study on the Phenomena of Prerotation at the Suction Side of Centrifugal Pumps," Irrigation and Power, No. 3, pp.381-390.

Miller, D.S., 1971, Internal Flow, A Guide to Losses in Pipe and Duct Systems. BHRA, Cranfield, England, p.58.

Paulon, J., Fradin, C. and Poulain, J., 1985, "Improvement of Pump Performance at Off-Design Conditions," ASME paper 85-GT-200.

Schiavello, B. and Sen, M., 1980 ,"On the Prediction of Reverse Flow Onset at the Centrifugal Pump Inlet," Performance Prediction of Centrifugal Pumps and Compressors, ASME, pp.261-272.

Tanaka, T., 1980, "An Experimental Study of Backflow Phenomena in a High Specific Speed Propeller Pump," ASME paper, 80-FE-6.